Measuring primordial non-Gaussianity through weak lensing peak counts

Marian, L ; Hilbert, S ; Smith, R E ; Schneider, P ; Desjacques, V

DOI: https://doi.org/10.1088/2041-8205/728/1/L13

The Astrophysical Journal Letters, 728:L13 (4pp), 2011 February 10 doi:10.1088/2041-8205/728/1/L13

MEASURING PRIMORDIAL NON-GAUSSIANITY THROUGH WEAK-LENSING PEAK COUNTS

Laura Marian[1], Stefan Hilbert[1], Robert E. Smith[1,2], Peter Schneider[1], and Vincent Desjacques[2]
[1] Argelander-Institut für Astronomie, Universität Bonn, Bonn, D-53121, Germany; lmarian@astro.uni-bonn.de
[2] Institute for Theoretical Physics, University of Zürich, Zürich, CH 8057, Switzerland
Received 2010 November 24; accepted 2010 December 28; published 2011 January 19

ABSTRACT

We explore the possibility of detecting primordial non-Gaussianity of the local type using weak-lensing peak counts. We measure the peak abundance in sets of simulated weak-lensing maps corresponding to three models $f_{\rm NL} = 0, -100$, and 100. Using survey specifications similar to those of EUCLID and without assuming any knowledge of the lens and source redshifts, we find the peak functions of the non-Gaussian models with $f_{\rm NL} = \pm 100$ to differ by up to 15% from the Gaussian peak function at the high-mass end. For the assumed survey parameters, the probability of fitting an $f_{\rm NL} = 0$ peak function to the $f_{\rm NL} = \pm 100$ peak functions is less than 0.1%. Assuming the other cosmological parameters are known, $f_{\rm NL}$ can be measured with an error $\Delta f_{\rm NL} \approx 13$. It is therefore possible that future weak-lensing surveys like EUCLID and LSST may detect primordial non-Gaussianity from the abundance of peak counts, and provide information complementary to that obtained from the cosmic microwave background.

Key words: early universe – galaxies: clusters: general – gravitational lensing: weak – large-scale structure of universe – methods: numerical

Online-only material: color figure

1. INTRODUCTION

The inflationary paradigm is the leading theory of the early universe, which is of fundamental interest for cosmology and particle physics. Understanding the mechanism and energy scale of inflation remain major goals yet to be attained, despite the continuous and fervent efforts invested in this field.

A measurement of primordial gravitational waves would pin down the energy scale of inflation, but this still belongs to the not-so-near future. One possible way to discriminate between single- and multi-field inflation models is to test the Gaussianity of the primordial density fluctuations (Creminelli & Zaldarriaga 2004). The cosmic microwave background (CMB) has been so far the main and cleanest inflationary probe. Recent results from the *Wilkinson Microwave Anisotropy Probe* (*WMAP*; Komatsu et al. 2011) suggested tentative 1σ-level evidence of primordial non-Gaussianity of the local type, defined by the equation

$$\Phi(\mathbf{x}) = \phi(\mathbf{x}) + f_{\rm NL}[\phi^2(\mathbf{x}) - \langle\phi^2(\mathbf{x})\rangle]. \quad (1)$$

The parameter $f_{\rm NL}$ quantifies the local quadratic deviation of the Bardeen potential Φ from a Gaussian potential ϕ, and it is currently constrained to the value 32 ± 21(Komatsu et al. 2011).

It has long been suggested (Grinstein & Wise 1986; Lucchin & Matarrese 1988; Fry & Scherrer 1994; Matarrese et al. 2000) that low-redshift observables can also be used to measure primordial non-Gaussianity, despite the fact that the density field at such redshifts is strongly non-Gaussian due to the action of gravity. In the local non-Gaussianity models, there are mainly two effects on low-redshift observables as recently outlined in the comprehensive study of Dalal et al. (2008), and further explored in Desjacques et al. (2009), Grossi et al. (2009), Pillepich et al. (2010), Lam & Sheth (2009), and Smith et al. (2010). First, $f_{\rm NL}$ induces a scale dependence in the bias of dark matter halos, which affects primarily the largest scales, i.e., $k < 0.02\,h\,{\rm Mpc}^{-1}$. Thus, one can in principle separate the $f_{\rm NL}$ scale dependence from the gravitational one, which occurs on smaller scales. Second, the abundance of massive halos is higher/lower for positive/negative values of $f_{\rm NL}$ (Matarrese et al. 2000; Lo Verde et al. 2008). As a final note, we emphasize the importance of high- and low-redshift constraints on non-Gaussianity as their comparison may provide insight into the scale dependence of $f_{\rm NL}$ (Byrnes et al. 2010; Shandera et al. 2010).

In this Letter, we shall numerically investigate the sensitivity of weak gravitational lensing (WL) peak counts to primordial non-Gaussianity of the local type. The potential of WL surveys to constrain $f_{\rm NL}$ has already been tackled (Amara & Refregier 2004; Pace et al. 2010; Fedeli & Moscardini 2010; Oguri & Takada 2011), though without considering shear peaks. Peak counts are a natural candidate for $f_{\rm NL}$ studies, since the largest of them are caused primarily by massive halos. For WL studies of peak statistics, we mention the works of Hamana et al. (2004), Hennawi & Spergel (2005), De Putter & White (2005), Marian et al. (2009), Kratochvil et al. (2010), Dietrich & Hartlap (2010), and Marian et al. (2010) and references therein. Should peak counts prove to be a sensitive $f_{\rm NL}$ probe, then one could easily use large future surveys like EUCLID (Refregier et al. 2010) or the Large Synoptic Survey Telescope (LSST; Abell et al. 2009) to obtain low-redshift constraints on primordial non-Gaussianity.

2. METHOD

The observable that we use is the convergence field, i.e., the matter density projected along the line of sight and scaled by a geometrical factor. We study simulated WL convergence maps created from ray tracing through a suite of *N*-body simulations, generated with the publicly available code GADGET (Springel 2005). A subset of these simulations was used and described in the work of Desjacques et al. (2009). Three values of $f_{\rm NL}$ are considered: 0, −100, and +100, while the other cosmological parameters are kept fixed. The cosmology matches the *WMAP* five-year data results (Komatsu et al. 2009). We have a total of 18 simulations, with six realizations per $f_{\rm NL}$ value. The initial conditions for each of the six sets of $f_{\rm NL}$-model realizations are matched to reduce the cosmic variance on the comparison of the peak functions corresponding to each model. The box size

is 1600 h^{-1} Mpc, the number of particles is $N = 1024^3$, and the softening length is $l_{\rm soft} = 40\,h^{-1}$ kpc.

We consider a survey similar to EUCLID (Refregier et al. 2010) and to LSST (Abell et al. 2009) for the WL simulations with an rms $\sigma_\gamma = 0.3$ for the intrinsic image ellipticity, a source number density $\bar{n}_{\rm gal} = 40\,{\rm arcmin}^{-2}$, and a redshift distribution of source galaxies given by $\mathcal{P}(z) = 1.5\,z^2/z_0^3\,\exp[-(z/z_0)^{1.5}]$, where $z_0 = 0.6$. The median redshift of this distribution is $z_{\rm med} = 0.86$.

From each N-body simulation we generate 16 independent fields of view. Each field has an area of $12 \times 12\,{\rm deg}^2$ and is tiled by 4096^2 pixels, yielding an angular resolution $\theta_{\rm pix} = 10$ arcsec and a total area of $\approx$14,000 deg^2 for each $f_{\rm NL}$ model. The effective convergence κ in each pixel is calculated by tracing a light ray back through the simulation with a Multiple-Lens-Plane ray-tracing algorithm (Hilbert et al. 2007b, 2009). Gaussian shape noise with variance $\sigma_\gamma^2/(\bar{n}_{\rm gal}\,\theta_{\rm pix}^2)$ is then added to each pixel, which creates a realistic noise level and correlation in the filtered convergence field (Hilbert et al. 2007a).

For the peak finding we use an aperture filter (Schneider 1996), matching an Navarro–Frenk–White (NFW) profile (Navarro et al. 1997) convolved with a Gaussian function. Thus, we adopt the convergence model $\kappa_{\rm model} = \kappa_{\rm NFW} \circ f_{\rm Gauss}$, where $f_{\rm Gauss}$ is a Gaussian function of width $f \times l_{\rm soft}$. Here $f = 1.5$ for $M < 7 \times 10^{14}\,h^{-1}\,M_\odot$, and $f = 2$ otherwise; the softening length $l_{\rm soft}$ was defined above. $\kappa_{\rm NFW}$ is the NFW convergence profile truncated at the virial radius, defined in Marian et al. (2010). This model agrees very well with the measured convergence profiles of the peaks in the maps. It is useful both when working with simulations, since it accounts for the lack of resolution below the softening scale, and when using real data, since shear data are difficult to obtain near the centers of clusters.

The amplitude of the smoothed field at a point $\mathbf{x_0}$ is given by

$$\hat{M}(\mathbf{x_0}) = \int d^2x\; W(\mathbf{x_0} - \mathbf{x})\kappa(\mathbf{x}), \tag{2}$$

where W is our filter and κ is the convergence field. The filter W can be written as follows:

$$W(x) = \mathcal{C}_{\rm w}\,\frac{\kappa_{\rm model}(x) - \bar{\kappa}_{\rm model}(R)}{\sigma_\gamma^2/\bar{n}_{\rm gal}}, \tag{3}$$

where $\mathcal{C}_{\rm w}$ is a normalization constant, R is the aperture radius, i.e., the radius over which the filter is compensated, and $\bar{\kappa}(x) = 2/x^2\int_0^x dy y\kappa(y)$. We choose the normalization constant to be

$$\mathcal{C}_{\rm w} = \frac{\sigma_\gamma^2}{\bar{n}_{\rm gal}}\,\frac{M_{\rm NFW}}{\int d^2x\,\kappa_{\rm model}^2(x) - \pi R^2\,\bar{\kappa}_{\rm model}^2(R)}\,. \tag{4}$$

If $\mathbf{x_0}$ is the location of a peak created by an NFW cluster of mass $M_{\rm NFW}$ and redshift z, and the convergence field is smoothed with a filter tuned to precisely such a cluster, i.e., $\kappa_{\rm model}$ in Equation (3) corresponds to the same $M_{\rm NFW}$ and z, then this filter returns a maximum signal-to-noise ratio (S/N) at $\mathbf{x_0}$. At this location, the amplitude of the smoothed map is

$$\hat{M}(\mathbf{x_0}|M_{\rm NFW}, z) = M_{\rm NFW}. \tag{5}$$

The peak is assigned the mass $M_{\rm NFW}$. If the peak does not correspond to a real halo, and it is the result of line-of-sight projections, then it can still be assigned an "effective" mass. In practice, we smooth the convergence field with filters of various masses, which yield different amplitudes (larger and smaller than the filter mass) at the location of peaks. We interpolate these amplitudes to determine the filter mass that would satisfy Equation (5).

We choose R to be the virial radius of the cluster to which the filter is tuned: $R = (3M_{\rm NFW}/800\,\pi\,\bar{\rho})^{1/3}$, where $\bar{\rho}$ is the mean density of the universe. Thus, a filter at a given redshift can be specified either through the mass $M_{\rm NFW}$ or through its size R. We adopt the mass convention of Sheth–Tormen (Sheth & Tormen 1999), with an overdensity defined as 200 $\times$ the mean density (not the critical density), and the concentration parameter of Gao et al. (2008). We evaluate the S/N of the mass estimator in a simplified scenario where we ignore projection effects and consider only the intrinsic ellipticity noise. In this case, the variance of the estimator is given by ${\rm Var}(\hat{M}) = M_{\rm NFW}\,\mathcal{C}_{\rm w}$, and the S/N is obtained by combining this with the above equations. Note that while the mass estimator does not depend on the shape noise due to the normalization constant $\mathcal{C}$, the S/N scales with it as aperture filters usually do: S/N $\sim (\bar{n}_{\rm gal}/\sigma_\gamma^2)^{1/2}$.

Finally, in the case where no shape noise is included, we use the same filter as in our previous work (Marian et al. 2010). This filter can also be obtained by formally taking $\sigma_\gamma^2/\bar{n}_{\rm gal} = 1$ in Equations (3) and (4) above.

The analysis of the convergence maps is carried out in two situations: with and without shape noise. We adopt a very conservative approach in which we consider known only the redshift distribution of the source galaxies and the shape noise level, without any other information on the sources or on the detected peaks. We also do not resort to tomographic techniques. While this is an overly pessimistic scenario for a next-generation lensing survey like EUCLID or LSST, our goal here is to provide a proof of concept of the possibility of using WL peak counts to constrain primordial non-Gaussianity, rather than the final quantitative answer to this question.

We perform a hierarchical smoothing of the maps with filters of various sizes, from the largest down to the smallest, as described in Marian et al. (2009, 2010). This approach removes the problem of "peaks-in-peaks" and it also naturally eliminates the dependence of the measured peak function on a particular filter scale. Since the median redshift of the source distribution is 0.86, we adopt a fixed redshift of 0.3 for the matched filter described above. For this redshift, the scale of the filter varies from corresponding masses of $2 \times 10^{15}\,h^{-1}\,M_\odot$ to $3 \times 10^{13}\,h^{-1}\,M_\odot$ in the absence of shape noise, and $10^{14}\,h^{-1}\,M_\odot$ in the presence of it. The latter lower-limit choice of the filter scale is due to the fact that shape noise contaminates seriously the smaller peaks; imposing a minimum S/N threshold alleviates but does not remove the contamination. Peaks are detected in the smoothed maps as local maxima and are assigned a mass as described above.

3. RESULTS

Figure 1 presents the main result of this work. The upper panels illustrate the peak functions measured in the $f_{\rm NL} = \pm 100$ cosmologies, in the absence (left panel) and presence of shape noise (right panel). For each $f_{\rm NL}$ model, the points are the average of the peak counts measured in all 96 fields and the error bars represent errors on the mean. In the case of shape noise, we select only peaks with an S/N > 3. We note that the two average peak functions are clearly distinct at the high-mass end, i.e., for $M > 3 \times 10^{14}\,h^{-1}\,M_\odot$. This is better seen in the lower panels

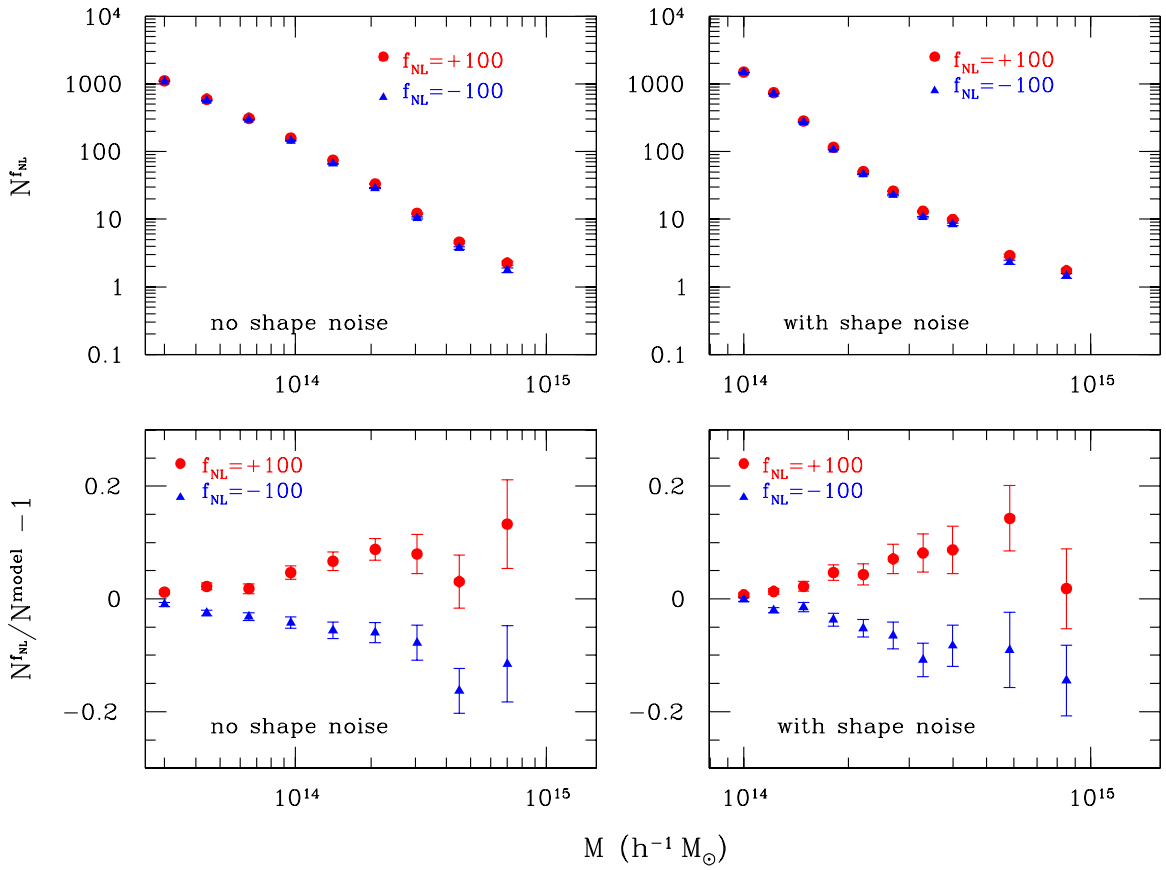

Figure 1. Upper panels: the measured peak functions for $f_{NL} = +100$ (red circles) and $f_{NL} = -100$ (blue triangles) for a survey with a median redshift $z_{med} = 0.86$, and an area of 14,000 deg^2. The filter used corresponds to redshift 0.3. The peak functions in the left panel are measured in the absence of shape noise, while in the right panel shape noise is included (assuming 40 galaxies arcmin^{-}2), and only the peaks with an S/N > 3 were selected (hence the smaller mass range on the *x*-axis). Lower panels: the fractional difference of the peak functions for the $f_{NL} = \pm 100$ models and the Gaussian model (red circles/blue triangles), without/with shape noise (left/right panel). The points are obtained as an average over all the fields of the fractional difference of the $f_{NL} \pm 100$ peak functions in every field and the average peak function in the Gaussian model.

(A color version of this figure is available in the online journal.)

which show the difference of the peak abundance measured in the $f_{NL} = \pm 100$ cosmologies, relative to the $f_{NL} = 0$ peak abundance. We have minimized the impact of the matched initial conditions of the simulations on the error bars: the fractional difference is computed as an average of the $f_{NL} \pm 100$ peak abundance in each field ratioed to the average Gaussian peak abundance of 96 fields (which represents our best model for the true Gaussian peak abundance), as opposed to the average of the ratio of the non-Gaussian and Gaussian peak functions measured in the same field. The latter would have removed the cosmic variance of the fractional difference, because of the matched initial conditions of the simulations from which we built the convergence maps.

Just like in the case of the three-dimensional halo mass function (see, for example, Desjacques et al. 2009; Smith et al. 2010), the peak functions for the f_{NL} models show a deviation from the Gaussian case. Unlike the three-dimensional studies which have presented halo mass functions measured at a single redshift, the peak functions that we show here combine peaks in the redshift range of the source distribution, and therefore are not as regular and symmetric as their three-dimensional counterparts. The asymmetry is most likely due to modifications of the S/N of peaks by line-of-sight projections and also by shape noise contamination. The trend is similar however, with high-mass peaks displaying the largest deviation. For both f_{NL} models, this is about 10%–15% for the largest mass bins, i.e., $M > 4 \times 10^{14}\,h^{-1}\,M_\odot$.

To quantify the significance of the deviation, we perform a χ^2-test. For the fiducial model $f_{NL} = 0$, we estimate the covariance of the counts in a field. We use the covariance of the mean to obtain the χ^2. For both $f_{NL} \pm 100$ we find a probability <0.1% to fit the $f_{NL} \pm 100$ peak functions with an $f_{NL} = 0$ peak function. This is also true if we consider only the diagonal elements (the variance of the mass bins) instead of the full covariance matrix, and also if we vary the mass bins. We also use the measured counts to estimate the Fisher error that a 14,000 deg^2 WL survey would yield on f_{NL}. Assuming all other cosmological parameters known, the forecasted error is $\Delta f_{NL} \approx 13$ for the fiducial value $f_{NL} = 0$. In the above we considered that the peak abundance scales linearly with f_{NL}, similar to the three-dimensional halo abundance. The values of the χ^2 and the Fisher error are largely maintained also if we minimize the impact of the matched initial conditions of the simulations, by using the first three simulations to compute the $f_{NL} = +100$ peak function and the last three for the $f_{NL} = -100$ function.

Though these results are already very encouraging, it is possible to improve measurements of primordial non-Gaussianity from WL surveys even if one considers only peak counts. The most important is probably the use of tomography, as numerical and analytical studies of the three-dimensional mass functions

have shown that deviations of the halo abundance from the Gaussian case significantly increase with redshift. Tomography would allow peaks to be separated not only in terms of their S/N–mass but also of their redshifts, thus acquiring more sensitivity to $f_{\rm NL}$. On the other hand, one has to beware a possible degeneracy with the amplitude of the matter power spectrum, σ_8. This can be solved by either using as a prior very good knowledge of σ_8 from other probes, such as the CMB (The Planck Collaboration 2006), WL, and large-scale structures or by combining several observables sensitive to both $f_{\rm NL}$ and σ_8, as exemplified in Oguri & Takada (2011). Our immediate goals are to further study how WL can be used to constrain primordial non-Gaussianity, to build improved $f_{\rm NL}$ estimators from WL observables, and to forecast $f_{\rm NL}$ constraints based on these observables.

For now we convey a simple, yet powerful statement: future WL surveys could detect primordial non-Gaussianity of the local type from at least one statistic-peak count. In particular, surveys like EUCLID and LSST should be able to provide complementary information to the $f_{\rm NL}$ information obtained from the ongoing CMB mission Planck (The Planck Collaboration 2006).

We kindly thank V. Springel for making public GADGET-2 and for providing his B-FoF halo finder. L.M., S.H., and P.S. are supported by the Deutsche Forschungsgemeinschaft (DFG) through the grant MA 4967/1-1, through the Priority Programme 1177 "Galaxy Evolution" (SCHN 342/6 and WH 6/3), and through the Transregio TR33 "The Dark Universe." R.E.S. and V.D. were partly supported by the Swiss National Foundation under contract 200021-116696/1, the WCU grant R32-2008- 000-10130-0, and the UZürich under contract FK UZH 57184001. R.E.S. also acknowledges support from a Marie Curie Reintegration Grant and the Alexander von Humboldt Foundation.

REFERENCES

Abell, P. A., et al. (LSST Science Collaborations) 2009, arXiv:0912.0201
Amara, A., & Refregier, A. 2004, MNRAS, 351, 375
Byrnes, C. T., Enqvist, K., & Takahashi, T. 2010, J. Cosmol. Astropart. Phys., JCAP09(2010)026
Creminelli, P., & Zaldarriaga, M. 2004, J. Cosmol. Astropart. Phys., JCAP10(2004)006
Dalal, N., Doré, O., Huterer, D., & Shirokov, A. 2008, Phys. Rev. D, 77, 123514
De Putter, R., & White, M. 2005, New Astron., 10, 676
Desjacques, V., Seljak, U., & Iliev, I. T. 2009, MNRAS, 396, 85
Dietrich, J. P., & Hartlap, J. 2010, MNRAS, 402, 1049
Fedeli, C., & Moscardini, L. 2010, MNRAS, 405, 681
Fry, J. N., & Scherrer, R. J. 1994, ApJ, 429, 36
Gao, L., Navarro, J. F., Cole, S., Frenk, C. S., White, S. D. M., Springel, V., Jenkins, A., & Neto, A. F. 2008, MNRAS, 387, 536
Grinstein, B., & Wise, M. B. 1986, ApJ, 310, 19
Grossi, M., Verde, L., Carbone, C., Dolag, K., Branchini, E., Iannuzzi, F., Matarrese, S., & Moscardini, L. 2009, MNRAS, 398, 321
Hamana, T., Takada, M., & Yoshida, N. 2004, MNRAS, 350, 893
Hennawi, J. F., & Spergel, D. N. 2005, ApJ, 624, 59
Hilbert, S., Hartlap, J., White, S. D. M., & Schneider, P. 2009, A&A, 499, 31
Hilbert, S., Metcalf, R. B., & White, S. D. M. 2007a, MNRAS, 382, 1494
Hilbert, S., White, S. D. M., Hartlap, J., & Schneider, P. 2007b, MNRAS, 382, 121
Komatsu, E., et al. 2009, ApJS, 180, 330
Komatsu, E., et al. 2011, ApJS, 192, 18
Kratochvil, J. M., Haiman, Z., & May, M. 2010, Phys. Rev. D, 81, 043519
Lam, T. Y., & Sheth, R. K. 2009, MNRAS, 398, 2143
Lo Verde, M., Miller, A., Shandera, S., & Verde, L. 2008, J. Cosmol. Astropart. Phys., JCAP04(2008)014
Lucchin, F., & Matarrese, S. 1988, ApJ, 330, 535
Marian, L., Smith, R. E., & Bernstein, G. M. 2009, ApJ, 698, L33
Marian, L., Smith, R. E., & Bernstein, G. M. 2010, ApJ, 709, 286
Matarrese, S., Verde, L., & Jimenez, R. 2000, ApJ, 541, 10
Navarro, J. F., Frenk, C. S., & White, S. D. M. 1997, ApJ, 490, 493
Oguri, M., & Takada, M. 2011, Phys. Rev. D, in press (arXiv:1010.0744)
Pace, F., Moscardini, L., Bartelmann, M., Branchini, E., Dolag, K., Grossi, M., & Matarrese, S. 2010, MNRAS, 1684
Pillepich, A., Porciani, C., & Hahn, O. 2010, MNRAS, 402, 191
Refregier, A., Amara, A., Kitching, T. D., Rassat, A., Scaramella, R., & Weller, J. (for the Euclid Imaging Consortium) 2010, arXiv:1001.0061
Schneider, P. 1996, MNRAS, 283, 837
Shandera, S., Dalal, N., & Huterer, D. 2010, arXiv:1010.3722
Sheth, R. K., & Tormen, G. 1999, MNRAS, 308, 119
Smith, R. E., Desjacques, V., & Marian, L. 2010, Phys. Rev. D, submitted (arXiv:1009.5085)
Springel, V. 2005, MNRAS, 364, 1105
The Planck Collaboration 2006, arXiv:astro-ph/0604069